

Influence of Polymer Characteristics and Melt-Spinning Conditions on the Production of Fine Denier Poly(Ethylene Terephthalate) Fibers. Part II. Melt Spinning Dynamics

CHANG T. KIANG* and JOHN A. CUCULO†

North Carolina State University, Fiber and Polymer Science, Raleigh, North Carolina 27695-8302

SYNOPSIS

The effect of poly(ethylene terephthalate) (PET) polymers with different rheological properties as well as the effect of different spinning conditions on the minimum attainable take-up denier were determined. The spinning conditions were modified by the use of heating devices, insulation plate, and convergence guides tested in the range of take-up speeds from 2000 to 6000 m/min. It is postulated that the important parameter in the production of fine denier PET fiber is the spinline tension level, which must be kept low in order to obtain finer denier fibers. The increase of take-up velocity and the threadline length increase the spinline stress level, and therefore the minimum denier attainable increases. The effect of the apparent elongational viscosity of the polymer and the threadline cooling profile can be thought as affecting the draw-down tension and therefore the minimum take-up denier. Higher apparent elongational viscosity level or faster cooling generates higher spinline tension resulting in higher minimum denier. The effects of the apparent elongational viscosity is more significant at a speed of 5000 m/min. This is in part due to the already very small denier obtained at speeds up to 4000 m/min, where the conditions of uniformity of polymer flow seem to be more important.

INTRODUCTION

The review of the data in the literature indicates that the main effect of decreased fiber denier is the faster cooling of the threadline due to the decreased mass throughput. From the present knowledge of the melt-spinning process, in particular in the more recent high-speed spinning process,¹ a high level of stress is expected in the spinline as a consequence of the fast cooling. Therefore the limit to the decrease of the fiber denier will be determined by the so-called cohesive fracture, i.e., fiber breakage when the local spinline stress exceeds the threadline strength.^{2,3}

The majority of publications reviewed in the literature studying fine denier fibers are concerned with their end-use properties, with some giving just

a basic description of the polymer processing conditions. Those few publications studying the fine denier production by the direct extrusion method, which is the main interest of the present research, are from the patent literature and give no specifics of the fiber formation mechanisms. Some exceptions are the paper by Qiu,⁴ which describes the effect of capillary diameter and quenching conditions, but for low spinning speeds less than 1500 m/min, and the theoretical calculation by Beyreuther et al.³ of the limits of the as-spun poly(ethylene terephthalate) (PET) fiber denier as a function of the threadline length and size of impurities in the polymer melt. Furthermore the structure and related properties of the fine denier fibers have not been extensively studied especially in connection with the dynamics of the threadline and the rheological properties of the PET polymer melt.

The present study is aimed at providing a more thorough understanding of the formation mechanism of the fine denier PET fiber obtained in high-speed melt spinning. The structure-property rela-

* Present address: Rhodia S.A., Sao Paulo, S.P., Brazil.

† To whom correspondence should be addressed.

tions will be the subject of a subsequent study. It is also the objective of this study to determine the minimum attainable denier in the as-spun fiber as a function of the take-up speed. Emphasis is given on the effects of the rheological properties of the PET polymer melts, characterized in the first paper,⁵ and the spinline modifications on the minimum attainable take-up denier.

EXPERIMENTAL

Materials

The PET polymers employed in the melt-spinning experiments are the same as those characterized in the first paper,⁵ as indicated in Table I.

Melt-Spinning Process

The melt-spinning equipment consists of a Fourne extruder with diameter $D = 22$ mm and ratio of the length L to diameter D equal to 25. A 0.3-cc/turn Zenith spin pump is employed to precisely control the polymer throughput in the spin block.

Two types of spin block were employed throughout the experiments, as shown in Figure 1. The majority of the experiments were done after the modifications in the spin block, which involved mainly a reduction of the size of the block with a more efficient heat transfer, a shorter path, and less stagnation points inside the block, improved temperature uniformity with the use of a static mixer, and pack modifications including an improved filtration step.

The spinneret plates have diameter D equal to 52 mm and thickness H equal to 14 mm. The number of holes in the spinneret varied, according to the experiment, from 1 to 14, and the capillary diameter varied from 0.15 to 0.23 mm. The ratio L/D of the length to the diameter of the capillaries is in the range of 2.3–2.5.

When applicable, a radial quench device (Q), 30 cm long, or heating device (HT), 20 cm long, were employed. These devices were fabricated at NCSU,

in which air is blown from outside to inside through a Fuji filter at a rate of 1.3 m/s in the quench device and 0.76 m/s in the heating device, measured at the center of the device bottom.⁶ The spinline cooling profile could also be modified with the use of a 4-cm-thick insulation plate, placed against the exit of the spinneret.

The extrudate can be taken up either by high-speed godet rolls (Erdmann Electrotechnik, maximum speed 8000 m/min) or by the Fourne winder (maximum speed 10,000 m/min). Take-up speeds from 2000 to 6000 m/min were used in the experiments. The threadline length varied in the range of 1.2–2.6 m, by moving either the extruder and/or the godet rolls.

The polymers were dried under vacuum at 140°C for at least 12 h prior to extrusion. The extrusion temperature was 295°C for the low intrinsic viscosity (IV) polymers (polymers A, B, C) and 310°C for the high IV polymer D.

On-line Measurements

A Zimmer noncontact diameter monitor, model 460 A/2, was employed to determine the threadline diameter profile. Improved reliability was obtained with the use of an analog-digital converter and storing the data in a computer. The diameter value is obtained from the peak of the distribution of 1000 acceptable data points. The acceptable data points are those with diameters less or equal to the spinneret capillary diameter.

The threadline stress was determined from the measurement of the total force acting on the multifilament bundle, with a three-point type Rothschild tensiometer of maximum load of 100 g and at a distance of 30 cm from the take-up point.

Threadline Dynamics

The spinline stress can be determined from the momentum balance on the threadline. For steady-state conditions, the following results are obtained.¹

$$F(x) = F(L^*) + w(V - V_L) + \pi\sigma(R_L - R_x) - \pi g \int_L^x \rho R_x^2 dx' + 2\pi \int_L^x R_x p_{xrs} dx' \quad (0 < x < L^*) \quad (1)$$

$$F(x) = F(L^*) - \pi g \rho R_L^2 (x - L^*) + 2\pi R_L p_{xrs}(L^*)(x - L^*) \quad (L^* < x < L) \quad (2)$$

Table I Characterization of the PET Samples

Sample	Supplier	IV	M_v
A	Goodyear	0.56	27,493
B	Rhone Poulenc A	0.64	33,784
C	Celanese	0.66	35,427
D	Goodyear	1.04	71,467

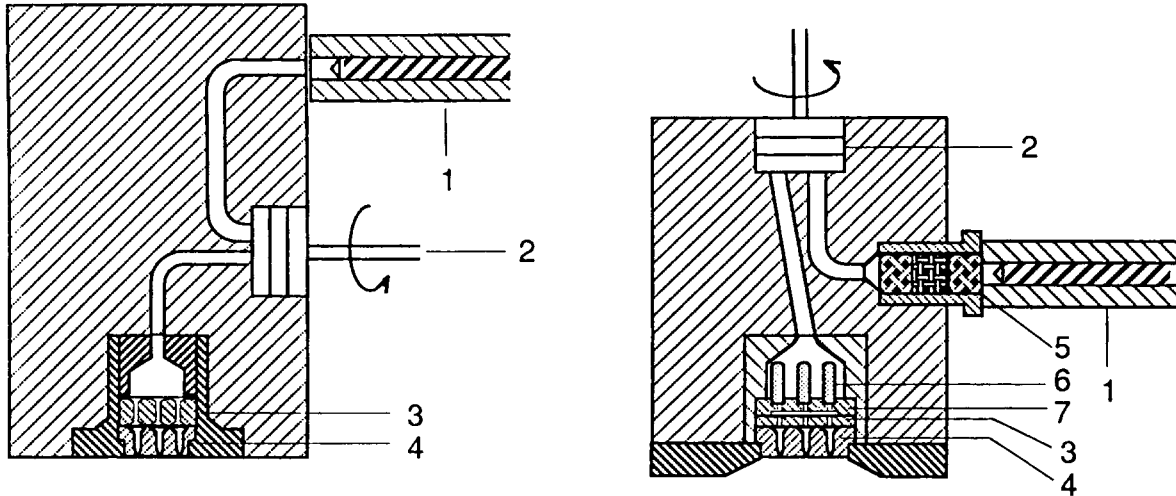


Figure 1 Schematic of the spin block: before modifications (left), after modifications (right). (1) extruder ($D = 22$ mm, $L/D = 25$); (2) spin pump; (3) breaker plate; (4) spinneret ($D = 52$ mm, $H = 14$ mm); (5) Koch static mixer KMB100 ($D = 1$ in., $L = 4$ in.); (6) Mott porous metal filters ($D = \frac{3}{8}$ in., $L = 1$ in.); (7) breaker plate/filter holder.

where w is the mass throughput per hole, V is the local axial velocity, R_x is the threadline radius at a distance x from the spinneret, L is the threadline length, L^* is the distance of the tension measurement point from the spinneret, $F(L^*)$ is the force measured with the tensiometer, ρ is the threadline density, g is the acceleration of gravity, σ is the surface tension coefficient and p_{xrs} is the shear stress on the filament surface due to air drag defined as follows:

$$p_{xrs} = C_f \rho_0 V^2 / 2 \quad (3)$$

where ρ_0 is the surrounding air density.

The air drag coefficient C_f can be calculated with the use of several correlations, compiled by Ziabicki.² The most often used correlations are listed below:

$$C_f = 0.37 \text{Re}_D^{-0.61} \quad (\text{Ref. 7}) \quad (4)$$

$$= 1.23 \text{Re}_D^{-0.81} \quad (\text{Ref. 8}) \quad (5)$$

The spinline stress is obtained from the definition

$$(p_{xx} - p_{rr})(x) = \frac{F(x)}{\pi R^2(x)} \quad (6)$$

Inertial forces are small in the spinning of fine denier fibers due to the low mass throughput w and so are the tension contributions from gravity. Surface tension effects are also small and can usually be neglected.

The experimental values of threadline diameter are fitted by a polynomial regression and used to calculate the threadline velocity. From the continuity equation, and assuming constant density:

$$w = \rho V(x) \pi R_x^2 = \rho V_L \pi R_L^2 \quad (7)$$

The spinline viscosity (SV) is defined as follows:

$$\text{SV}(x) = \frac{(p_{xx} - p_{rr})(x)}{dV(x)/dx} \quad (8)$$

where $dV(x)/dx$ is the velocity gradient at a distance x from the spinneret, obtained from the slope of the threadline velocity profile plots.

Birefringence

Birefringence measurements were determined with a Nikon polarizing microscope and a Leitz tilting compensator (model E, 20 orders). The results are an average of the measurement of 10 individual fibers.

Take-up Denier

The take-up denier (dpf) can be calculated either from the knowledge of the polymer throughput in the spinneret hole or from the measurements of the diameter of the fiber under the microscope.

$$\text{dpf} = 9.4366 \times 10^{-3} d_L^2 \quad (9)$$

$$= 9000W/(nV_L) \quad (10)$$

The coefficient in Eq. (9) is obtained for values of fiber diameter d_L in microns, and assuming fiber density equal to 1.335 g/cm^3 . In Eq. (10), n is the number of holes in the spinneret and W is the total mass throughput. Unless otherwise noted, the take-up denier reported in this work is obtained from Eq. (10).

RESULTS AND DISCUSSIONS

Effect of Polymer and Spinning Conditions on the Minimum Attainable Take-up Denier

The initial tests to determine the minimum attainable denier of the as-spun fibers were conducted with polymers A (low IV) and D (high IV). The polymers were extruded at 295°C (low IV) and 310°C (high IV) through a $7 \times 0.18 \text{ mm}$ ($L/D = 2.3$) spinneret, without quenching or heating. Two threadline lengths were used, 1.2 and 2.4 m, and the fibers were spun at three take-up speeds, 2000, 3000, and 5000 m/min.

The results of the minimum denier achievable under each spinning condition are shown in Figure 2. It can be seen that the low IV polymer allows the spinning of finer denier fibers. It is also shown in this figure that the shorter threadline allows finer denier fibers to be spun. As discussed in an earlier

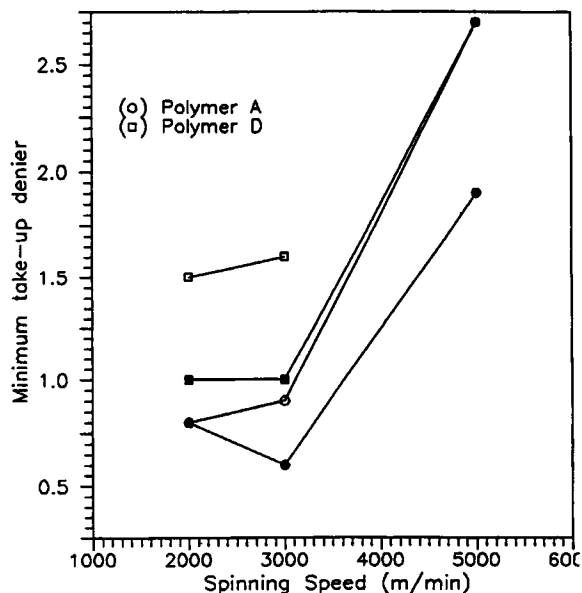


Figure 2 Minimum as-spun denier as a function of take-up speed. Polymers A ($T = 295^\circ\text{C}$) and D ($T = 310^\circ\text{C}$), sp. $7 \times 0.18 \text{ mm}$ ($L = 2.3D$), without quench/heating, $L = 1.2 \text{ m}$ (filled symbols), $L = 2.4 \text{ m}$ (unfilled symbols).

study,⁵ the values of the minimum denier obtained at spinning speeds below 3000 m/min are also affected by the flow conditions inside the pack. These conditions become critical at the low take-up speed range due to the very small throughputs involved in our experimental apparatus. The value of the minimum take-up denier increases significantly at 5000 m/min compared to those at lower speeds. The high IV polymer could not be spun at 5000 m/min with the longer threadline due to limitation in the spin pump maximum speed.

Figure 3 shows the corresponding results of birefringence. The threadline length has negligible influence on the birefringence, which may indicate that the deformation region in the spinline is unaffected by the change of the threadline length in the range of 1.2–2.4 m. The high IV polymer results in a higher birefringence as expected, but the difference is considerably reduced at the speed of 5000 m/min.

The modifications made in the spin block, as shown in Figure 1, resulted in better polymer uniformity. The improved uniformity is presumed to be due to a more uniform melt temperature after the mixing device, as well as better filtration in the extended porous filters as compared to the metal screens used formerly. A better uniformity is also expected among the capillaries of the spinneret due to better flow distribution from the simultaneous use of the porous filter and breaker plate. Figure 4 shows the considerable reduction of the minimum take-up denier for polymer A with the new pack compared to the previous results obtained under similar spinning conditions.

The results that will be presented subsequently were obtained with the new pack. Note also that spinnerets with 14 holes uniformly distributed on the plate surface replace the formerly used spinnerets with 7 holes arranged in one circle along the outer edge of the plate.

Figure 5 shows that the minimum take-up denier increases dramatically when the take-up velocity is increased from 4000 to 5000 m/min. At the speed range below 3000 m/min, the minimum denier is again affected by the polymer flow distribution inside the pack, as discussed previously in the results of Figure 2. For speeds greater than 4000 m/min and particularly at 5000 m/min the smallest value of minimum take-up denier, at a given spinning speed, is obtained with polymer A followed by polymer C and then polymer B.

The effect of the threadline length and take-up speed on the minimum attainable denier, shown in Figures 2 and 4, are in qualitative agreement with the theoretical calculations by Beyreuther.³ As

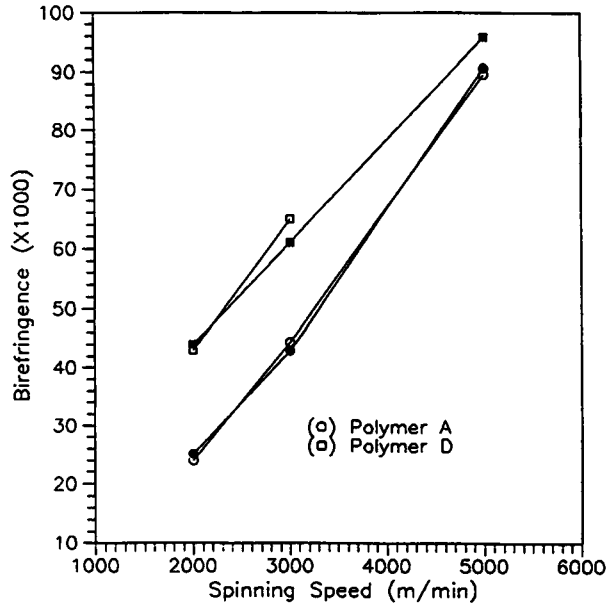


Figure 3 Birefringence as a function of take-up speed. Polymers A ($T = 295^{\circ}\text{C}$) and D ($T = 310^{\circ}\text{C}$), sp. 7×0.18 mm ($L = 2.3D$), without quench/heating, $L = 1.2$ m (filled symbols), $L = 2.4$ m (unfilled symbols).

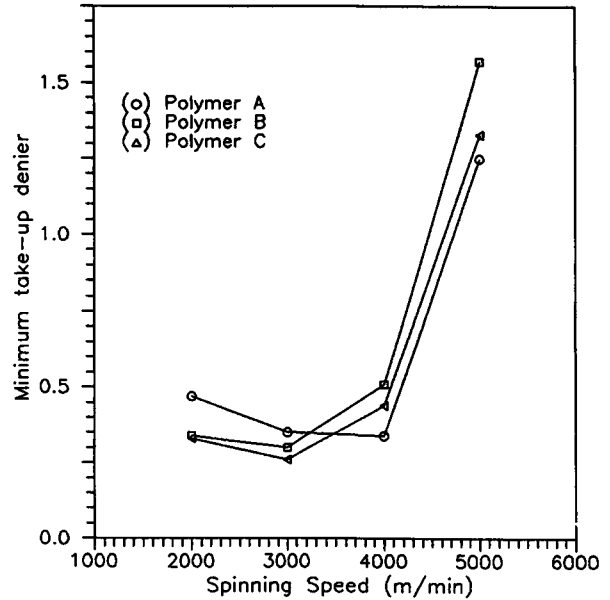


Figure 5 Minimum as-spun denier as a function of take-up speed and different PET polymers. $T = 295^{\circ}\text{C}$, sp. 14×0.23 mm ($L = 2.5D$), $L = 2.6$ m, without quench/heating.

shown in Figures 6 and 7, take-up stress increases with increase of take-up speed and threadline length, and even faster with decrease of the take-up denier. The increase of the take-up stress can be explained from the increase of the cooling rate and the increase

of air drag, as will be shown by the analysis of the threadline dynamics. The take-up stress should be reduced in order to obtain finer denier fibers.

Figures 8 and 9 show the threadline velocity pro-

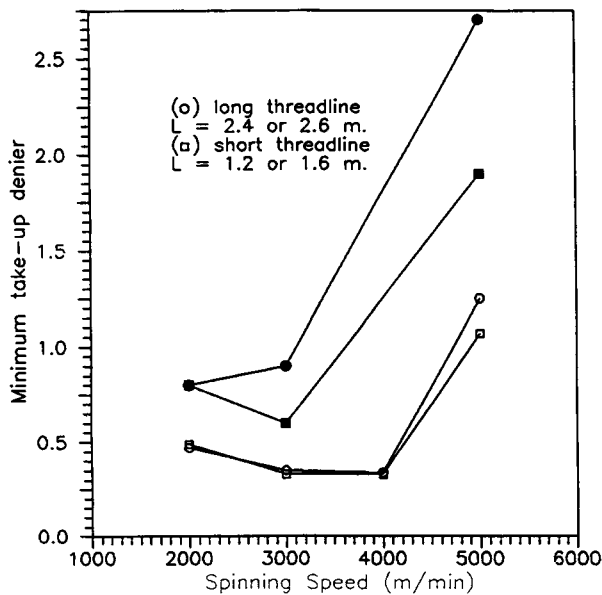


Figure 4 Effect of spin pack modifications, as shown in Figure 1, on the minimum as-spun denier of polymer A as a function of take-up speed. Filled symbols: before modifications.

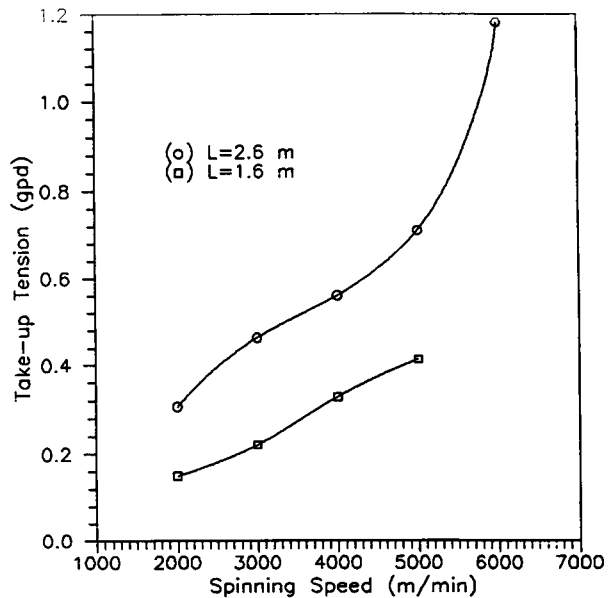


Figure 6 Take-up stress of polymer A as a function of take-up speed. $T = 295^{\circ}\text{C}$, sp. 14×0.23 mm ($L = 2.5D$), without quench/heating (for $V_L > 5000$ m/min, insulation plate and convergence guide used), dpf = 1.00 (dpf = 1.25 at $V_L = 5000$ m/min).

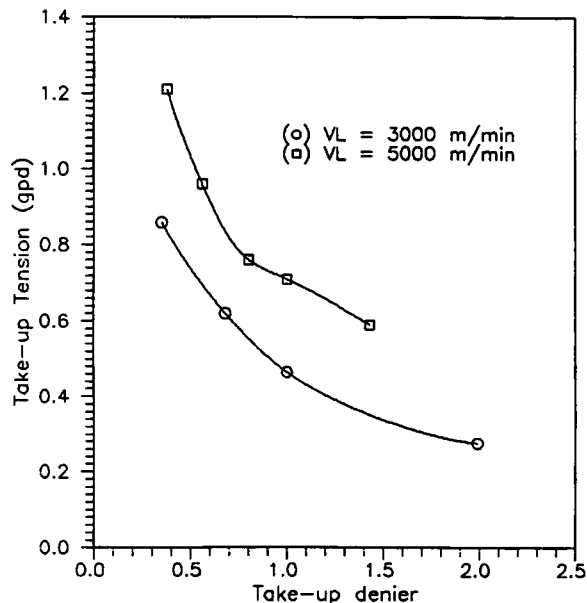


Figure 7 Take-up stress of polymer A as a function of take-up denier. $T = 295^{\circ}\text{C}$, sp. $14 \times 0.23 \text{ mm}$ ($L = 2.5D$), $L = 2.6 \text{ m}$, without quench/heating (insulation plate and convergence guide used at $V_L = 5000 \text{ m/min}$).

file calculated from the measured threadline diameter profile, taken with the Zimmer monitor. Figures 10 and 11 show the respective calculated threadline velocity gradient profiles. The velocity profiles in

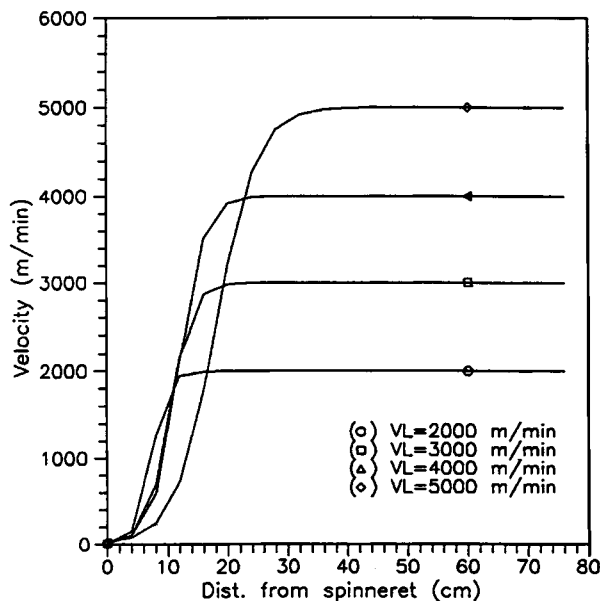


Figure 8 Threadline velocity profile (calculated) of polymer A at different take-up speeds. $T = 295^{\circ}\text{C}$, sp. $14 \times 0.23 \text{ mm}$ ($L = 2.5D$), $L = 2.6 \text{ m}$, without quench/heating, dpf = 1.00 (dpf = 1.25 at $V_L = 5000 \text{ m/min}$).

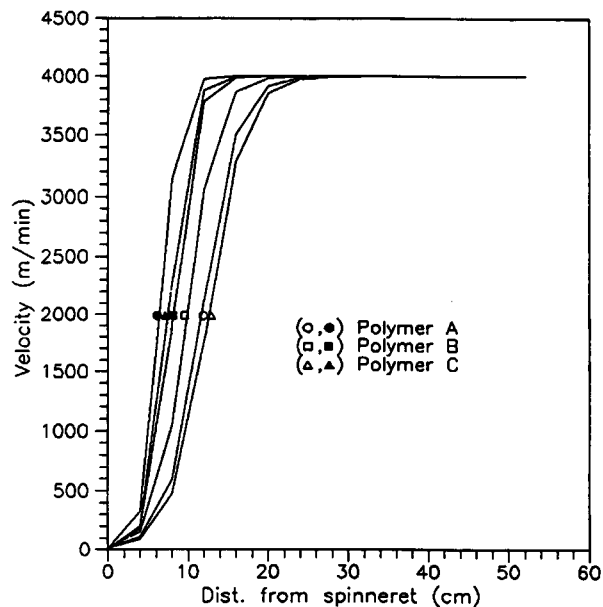


Figure 9 Threadline velocity profile (calculated) of different PET polymers. $T = 295^{\circ}\text{C}$, sp. $14 \times 0.23 \text{ mm}$ ($L = 2.5D$), $L = 2.6 \text{ m}$, without quench/heating, $V_L = 4000 \text{ m/min}$, dpf = 1.00 (unfilled symbols); minimum denier (filled symbols).

Figure 8 correspond to fibers from polymer A spun at different take-up speeds and constant denier equal to 1, except at 5000 m/min where the denier was

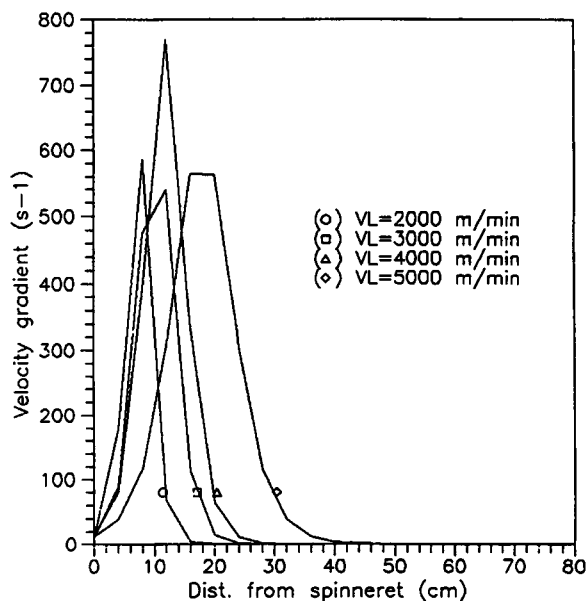


Figure 10 Threadline velocity gradient profile (calculated) of polymer A at different take-up speeds. $T = 295^{\circ}\text{C}$, sp. $14 \times 0.23 \text{ mm}$ ($L = 2.5D$), $L = 2.6 \text{ m}$, without quench/heating, dpf = 1.00 (dpf = 1.25 at $V_L = 5000 \text{ m/min}$).

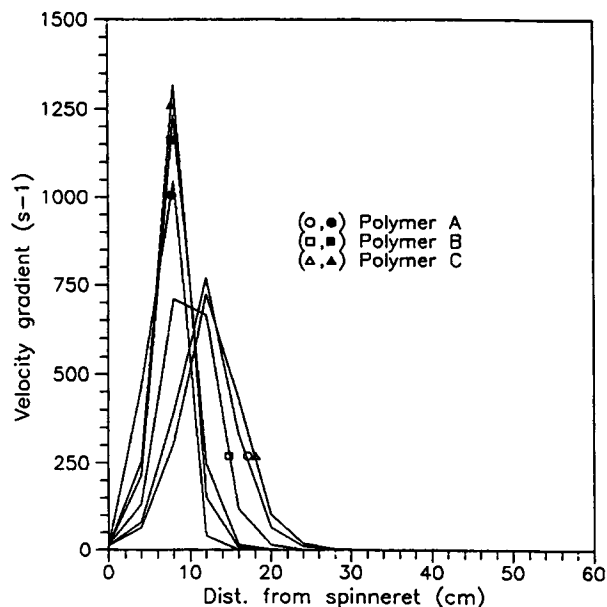


Figure 11 Threadline velocity gradient profile (calculated) of different PET polymers. $T = 295^{\circ}\text{C}$, sp. 14×0.23 mm ($L = 2.5D$), $L = 2.6$ m, without quench/heating, $V_L = 4000$ m/min, dpf = 1.00 (unfilled symbols); minimum denier (filled symbols).

equal to 1.25. It can be seen that the position at which the fiber reaches its final velocity, when the denier is kept constant, is displaced to greater distance from the spinneret as the take-up speed increases. The same behavior is observed for the peak of the velocity gradient, as shown in Figure 10. Since the final denier is approximately the same in all cases, it is expected that at higher take-up speeds the cooling rate is slower due to the higher mass throughput. This is in accord with the theoretical calculation by Ziabicki.¹ The velocity profiles for the three low IV polymers spun at 4000 m/min are shown in Figure 9. The measured profiles for the 1-denier fibers as well as those for the minimum denier of each polymer at this speed are shown. The cooling of the finest fibers is even faster, reaching the final velocity at less than 20 cm from the spinneret. At constant denier equal to 1 dpf, polymer B presents the fastest increase of velocity. For the finest denier fibers, the smaller the denier the faster is the change in the threadline velocity. Figure 11 shows that the maximum velocity gradient values for the 1-denier fibers spun at 4000 m/min equal 750 s^{-1} whereas those of the finest deniers are much larger, ranging from 1000 to 1300 s^{-1} .

Figures 4 and 5 indicate that the minimum attainable denier remains almost unchanged for take-up speeds up to 4000 m/min, even though the take-

up stress continues to increase. The approximately unchanged value of the minimum denier for take-up speeds lower than 4000 m/min indicates the existence of a proportionality between the increase of the take-up stress and the fiber strength as the spinning velocity is increased. At 5000 m/min the take-up stress overpasses the fiber strength so that the minimum denier value increases. In the theoretical calculation of the minimum denier, Beyreuther³ assumed a constant fiber strength, and therefore his result showed a continuous increase of the minimum denier with the increase of take-up speed, in contradiction to our experimental observations.

Up to 3000 m/min the values of the minimum denier are very low, and the observed differences among the three low IV polymers are mainly due to the conditions of polymer flow distribution in the pack. The flow conditions inside the pack are critical at the low take-up speed range due to the very small throughputs involved. This is confirmed by the significant reduction of the minimum attainable denier after the modifications made to the spin block, shown in Figure 4, which resulted mainly in improvements of the polymer uniformity and flow distribution inside the pack.

At take-up speeds above 4000 m/min, it has been observed that the smallest value of minimum take-up denier, under similar spinning conditions as shown in Figure 5, is obtained with polymer A, followed by polymers C and B. This sequence coincides with the sequence of decreasing level of apparent elongational viscosity, as determined in the previous paper⁵ for these polymers. The most remarkable of these results is that for polymers with similar shear viscosity (polymers B and C), the polymer with lower apparent elongational viscosity (polymer C) can be spun to a lower denier. The same conclusion applies to polymers with different shear viscosities as observed between polymer A and the two other low IV polymers B and C, or the high IV polymer D as shown earlier in Figure 2, the key parameter being the level of the apparent elongational viscosity. This is consistent with the conclusions reached by Laun and Schuch⁹ on the effect of the elongational viscosity on the maximum draw-down speeds.

The correlation between the level of the apparent elongational viscosity determined in contraction flow and the minimum attainable denier can be explained in terms of its effect on the threadline stress level and cooling profile. It seems reasonable to speculate that the higher level of apparent elongational viscosity generates higher draw-down tension and therefore faster diameter attenuation and increased cooling of the threadline. A shorter solidi-

fication distance gives rise to an increase of the air friction component of the stress, which contributes the major portion to the threadline stress. As discussed earlier, the increase of the threadline stress limits the value of the minimum attainable denier by the mechanism of cohesive fracture.^{2,3}

Determination of the Optimum Spinneret Capillary Diameter

The effect of spinneret capillary diameter was studied with spinnerets with capillary diameter of 0.23, 0.18, and 0.15 mm. All 3 spinnerets have 14 holes and L/D equal to 2.5. The tests were conducted with polymer B.

Figure 12 shows the effect of the spinneret capillary diameter on the minimum attainable take-up denier at different take-up speeds. The capillary diameter has no effect on the minimum denier up to a speed of 3000 m/min. At 4000 m/min, the 0.15-mm capillary allows spinning of the lowest denier fiber, with the extraordinary value of 0.22 dpf, whereas at 5000 m/min the 0.18-mm capillary gives the finest fiber.

The conclusion from these results is that smaller capillary diameter is required to obtain finer fibers at high spinning speeds. The smaller capillary diameter reduces the draw ratio between the spinneret and winder, avoiding the fast attenuation of the fiber at the exit of the spinneret that would otherwise

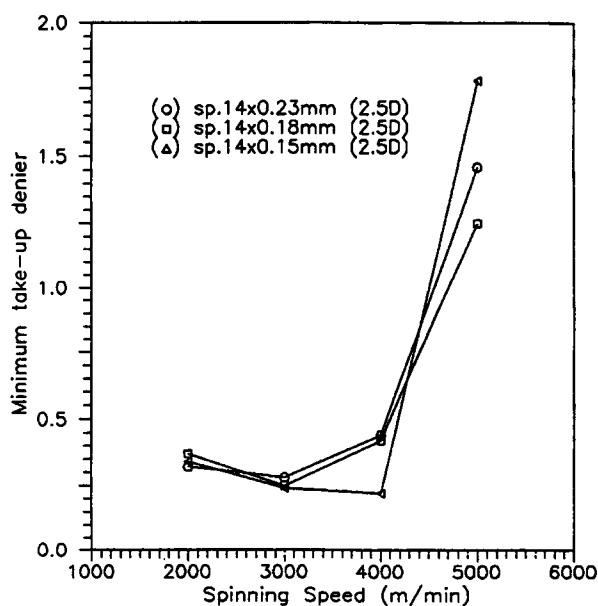


Figure 12 Minimum as-spun denier of polymer B as a function of take-up speed and different spinnerets. $T = 295^\circ\text{C}$, $L = 2.6$ m, without quench/heating.

occur. However, the higher throughputs involved in the higher take-up speeds require that the optimum capillary diameter be increased in order to lower the shear rate at the spinneret. These results can be quantitatively explained from the relations of the shear rate (ϵ_s) and draw down ratio (DDR) to the spinneret capillary diameter.

$$\epsilon_s = a8V_0/d_0 \quad (11)$$

$$\text{DDR} = V_L/V_0 \quad (12)$$

where a is the Rabinowitsch correction, V_0 is the velocity at the exit of spinneret, and V_L is the take-up velocity.

From the continuity equation:

$$w = \text{constant} = \frac{\rho_0 V_0 \pi d_0^2}{4} = \frac{\rho_L V_L \pi d_L^2}{4} \quad (13)$$

where w is the mass throughput per hole and ρ_0 , ρ_L is polymer density at the exit of spinneret and at the take-up, respectively.

The diameter of the fiber at the take-up device (d_L) is related to the take-up denier (T_d) by

$$T_d = k\rho_1 d_L^2 \quad (14)$$

Substituting (14) in (13) and rearranging,

$$V_0 = (k'/\rho_0)(T_d/d_0^2)V_L \quad (15)$$

Substituting (15) in (11) and (12), one obtains

$$\epsilon_s = KT_d V_L/d_0^3$$

$$\text{DDR} = K'd_0^2/T_d$$

From these relations one can see that the capillary diameter d_0 has an opposite effect on the shear rate at the capillary and the draw down ratio, for a given take-up denier and velocity. Decreasing the diameter of the capillaries, increases the shear rate and decreases DDR. The capillary diameter should be reduced when the fiber denier decreases to keep, respectively, the shear rate and DDR constant. Table II presents the results of the calculations of the shear rate and draw-down ratio for the cases of the lowest values of take-up denier, spun at 4000 and 5000 m/min, including the results to be described in the following section.

Table II indicates the existence of a narrow range for the optimum value of the shear rate and draw-down ratio, based on the results of the finest denier

Table II Optimum Shear Rate (ϵ_s) and Draw-Down Ratio (DDR) for the Finest Denier Fibers

Take-up Speed (m/min)	Capillary Diameter	Minimum Denier	ϵ_s (s^{-1})	DDR
4000 (polymer B)	0.15 mm	0.22 ^a	4200	860
	0.18 mm	0.42	4600	650
	0.23 mm	0.44	2300	1020
5000 (polymer A)	0.18 mm	0.38 ^a	5250	710
	0.23 mm	0.56 ^a	3700	790
5000 (polymer B)	0.15 mm	1.78	41600	110
	0.18 mm	1.25	16800	220
	0.23 mm	1.46	9400	310

^a Finest denier fibers obtained in this study, at each respective take-up speed.

fibers obtained in all experiments done in the present research. The optimum shear rate range is shown to be $4\text{--}5 \times 10^3 \text{ s}^{-1}$ while the optimum draw down ratio is in the range $7\text{--}9 \times 10^2$. The existence of an optimum range for the shear rate and draw-down ratio indicates that the optimum capillary diameter is a function of the take-up speed and denier. The range of the capillary diameter used throughout these experiments, from 0.15 to 0.23 mm, is in the same range cited in other works.^{4,10-12}

Effect of Various Spinline Modifications on the Minimum Attainable Take-up Denier

The results in Figures 2, 4, 5, and 12 show that the minimum attainable take-up denier can be reduced by improving the uniformity of the polymer melt in the spin block, reducing the length of the threadline, employing polymers with lower apparent elongational viscosity, and selecting the optimum capillary diameter. However, at spinning speeds above 4000 m/min, take-up denier below 1 dpf is hardly obtained with the cited improvements.

Since the limit of the minimum attainable denier is determined by the mechanism of cohesive fracture, as discussed earlier, it is expected that, by reducing the threadline stress level through modifications of the spinline, the minimum attainable denier might also be reduced. The spinline was modified by introduction of a heating device, insulation plate, and convergence guide. Two spinnerets were used, $14 \times 0.23 \text{ mm}$ ($L = 2.5D$) and $14 \times 0.18 \text{ mm}$ ($L = 2.5D$). No quench was utilized and the threadline length was 2.6 m. The take-up speed was 5000 m/min throughout the experiments, since at this speed dpf below 1 is more difficult to obtain. The insulation plate was 4 cm thick and the convergence guide was placed 70 cm from the spinneret.

Tables III and IV summarize the different spinning conditions employed and the resulting take-up denier and birefringence. The lowest value of denier at each spinning condition represents the minimum value attainable. Referring to Table IV, for each polymer the value of the denier when no devices are used corresponds to the minimum denier attainable. As an example, the minimum attainable denier for polymer B, when no devices are used, is 1.76 dpf. When an insulation plate and convergence guide are used, the minimum becomes 0.95 dpf. However, in order to compare with the condition where no devices were used, it was necessary also to include the condition of 1.76 dpf. Similarly, the condition of 1.43 dpf was included to allow comparison of all three polymers (see Table III) at the same dpf. The same reasoning applies to the results of polymer C, shown in Table IV.

The results from Tables III and IV show that the simultaneous use of the convergence guide and insulation plate is the most efficient way to lower the minimum attainable take-up denier. It is also shown that the use of the heating device 15 cm from the spinneret and a temperature of 180°C is less effective in reducing the minimum denier than the use of the convergence guide alone. No significant improvement is observed when the convergence guide is used together with a heating device. The insulation plate is the most effective single device to reduce the minimum denier, which is further improved when used in combination with the convergence guide.

The finest denier was obtained with polymer A, followed by polymers C and B, when compared under similar spinning conditions. These results confirm those presented earlier and coincide with the sequence of increasing level of the calculated apparent elongational viscosity of these polymers. One important result is that for all three low IV PET poly-

Table III Summary of the Different Spinning Conditions (Polymer A)^a

Heater	Ins. plate	Conv. Guide	Denier	Biref. ($\times 10^3$)
Polymer A, sp. 14×0.23 mm ($L = 2.5 D$), filter $50 \mu\text{m}$				
N	N	N	1.43	91.4
$Z = 15/T = 180$	N	N	1.43	87.7
			1.21	88.5
$Z = 15/T = 160$	N	Y	1.12	89.8
	N	Y	1.43	83.6
			0.92	87.0
N	N	Y	1.43	81.2
			1.08	86.1
N	Y	Y	1.43	84.0
			0.56	89.0
Polymer A, sp. 14×0.18 mm ($L = 2.5 D$), filter $20 \mu\text{m}$				
N	N	N	1.43	88.5
N	Y	Y	1.43	88.2
			0.38	98.0

^a Y = device used. N = device not used.

mers, it is possible to obtain fibers spun at 5000 m/min with denier below 1, with the simultaneous use of the insulation plate and convergence guide. It is also the first time that we could obtain fibers spun at 5000 m/min with the remarkable result of 0.38 denier. This was possible using the spinneret capillary diameter of 0.18 mm, which was shown to be the optimum capillary diameter when spinning at 5000 m/min. Also improved polymer filtration in the spin pack, by using a porous metal filter with a

nominal grade of $20 \mu\text{m}$, instead of $50 \mu\text{m}$ normally used, had a beneficial effect. This fiber, obtained with the described change in the pack system along with the use of the insulation plate and convergence guide, showed also high value of birefringence of ca. 0.100.

The use of a convergence guide at distances from 50 to 300 cm from the spinneret is frequently cited in the Japanese patent literature.^{10,11,13-17} However, the simultaneous use of an insulation plate, to protect

Table IV Summary of Different Spinning Conditions. Polymers B and C^a

Heater	Ins. plate	Conv. Guide	Denier	Biref. ($\times 10^3$)
Polymer B, sp. 14×0.23 mm ($L = 2.5 D$), filter $50 \mu\text{m}$				
N	N	N	1.76	79.4
N	Y	Y	1.76	78.4
			1.43	79.8
			0.95	82.6
Polymer C, sp. 14×0.23 mm ($L = 2.5 D$), filter $50 \mu\text{m}$				
N	N	N	1.62	87.1
N	Y	Y	1.62	87.4
			1.43	88.6
			0.80	90.3

^a Y = device used. N = device not used.

the face of the spinneret, and a convergence guide was cited only by Asahi^{14,15} where they used a 1-cm-thick asbestos sheet and convergence guide 10–200 cm from the spinneret. The spinning speed used, however, was only 1250 m/min, and air was blown against the insulation to keep the temperature below the spinneret below 200°C. In the present study an insulation plate 4 cm thick was used and a convergence guide was placed 70 cm from the spinneret for spinning speeds in excess of 5000 m/min.

The spinline diameter profiles were measured with the Zimmer noncontact diameter monitor and used to calculate the threadline velocity profile shown in Figures 13 and 14. The quantitative results of these calculations are limited by the scarcity of diameter data points in the deformation zone due to the very fast cooling mentioned earlier. Even in the case when a heating device is used and the cooling is slower, few data points are attainable since the diameter data are not available in the heater zone. The results with polymer A are presented in Figure 13, comparing the effect of several spinline modifications on the threadline velocity profile as well as the effect of a lower denier. In this figure N indicates that a device is not used and Y indicates that the device is used. Figure 14 compares the threadline velocity profile results for the three poly-

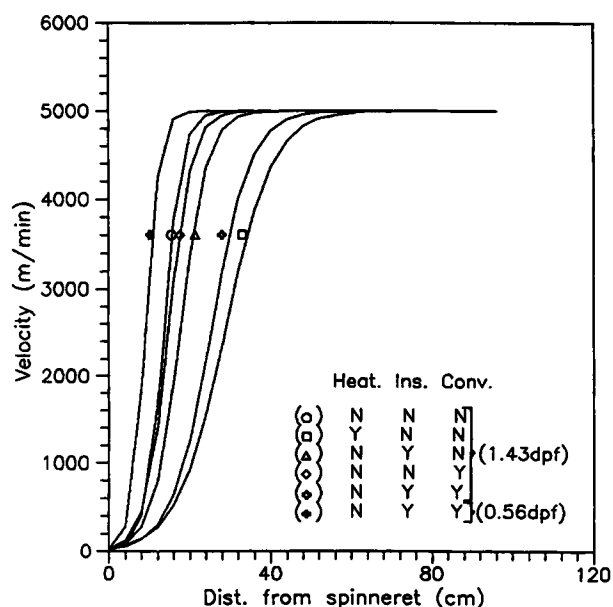


Figure 13 Threadline velocity profile (calculated) of polymer A with varying spinline modifications. $T = 295^\circ\text{C}$, sp. 14×0.23 mm ($L = 2.5D$), $L = 2.6$ m, without quench, heating ($H = 20$ cm, $Z = 15$ / $T = 180^\circ\text{C}$), insulation plate (4 cm thick), convergence guide ($l = 0.7$ m), $V_L = 5000$ m/min.

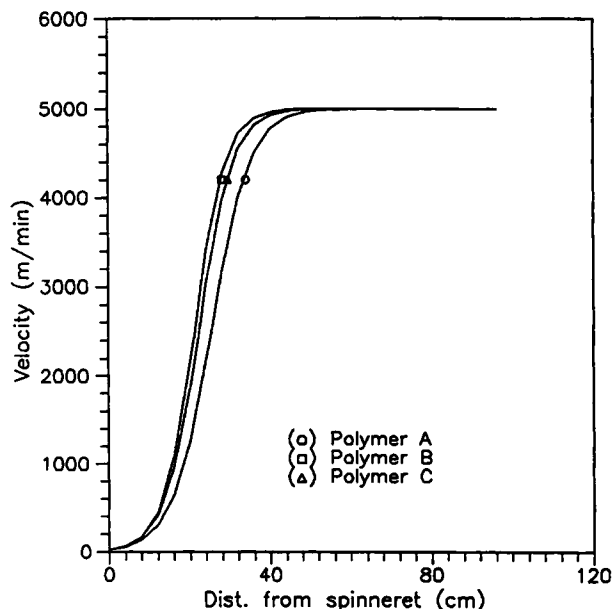


Figure 14 Threadline velocity profile (calculated) of different PET polymers. $T = 295^\circ\text{C}$, sp. 14×0.23 mm ($L = 2.5D$), $L = 2.6$ m, without quench/heating, insulation plate (4 cm thick) plus convergence guide ($l = 0.7$ m), $V_L = 5000$ m/min, $\text{dpf} = 1.43$.

mers under the same spinning conditions and take-up denier.

Figure 13 shows the effect of the heating device, insulation plate, and convergence guide, when used individually or simultaneously, at constant take-up denier as well as different take-up denier, on the threadline velocity profile. The use of a convergence guide 70 cm from the spinneret slows down the spinline cooling. This effect of delaying quench is increased when an insulation plate is used, and even more with the heating device. Except for the case of the heating device, in all cases the fiber reaches final velocity at a distance less than 40 cm from the spinneret. The cooling rate is reduced with the simultaneous use of the insulation plate and convergence guide but not as much as when only the heating device is used. The lower denier fiber solidifies at less than 20 cm from the spinneret.

Figure 14 compares the threadline velocity profile of the fibers spun from the three low IV PET polymers, at the constant denier of 1.43 and with the simultaneous use of the insulation plate and convergence guide. Fibers from polymer B show the fastest cooling, followed by polymers C and A. This is again the same sequence for the decreasing limit of the minimum denier and decreasing level of the apparent elongational viscosity.

The velocity profile data allow us to calculate the

velocity gradient profiles shown in Figures 15 and 16. The maximum velocity gradient values range from 300 to 1200 s^{-1} . These values are within the range of the apparent elongational viscosity data calculated from the Instron rheometer experiments, presented in the earlier paper.⁵ The velocity gradient peak increases and moves closer to the spinneret with faster cooling. This indicates higher accelerations in the threadline and maximum deformations closer to the spinneret as the cooling rate is increased. The velocity gradient data will be further used in the estimation of the spinline viscosity.

The spinline stress data are shown in Figures 17 and 18. In order to magnify the differences in the solidification region, the air friction coefficient from the Kase and Matsuo correlation,⁸ Eq. (5), was modified to

$$C_f = 0.37 \text{Re}^{-0.81}$$

This should not interfere in our conclusions since the primary interest resides in the analysis of the qualitative effects of the spinline modifications and comparison between polymers. A more quantitative analysis would be of little value due to the uncertainties in the calculation of the velocity profiles. Additionally, no attempt was made to correct the

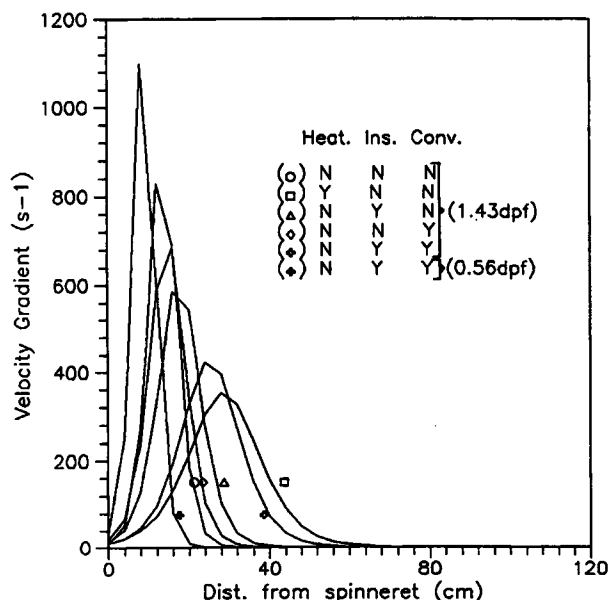


Figure 15 Threadline velocity gradient profile (calculated) of polymer A with varying spinline modifications. $T = 295^\circ\text{C}$, sp. 14×0.23 mm ($L = 2.5D$), $L = 2.6$ m, without quench, heating ($H = 20$ cm, $Z = 15/T = 180^\circ\text{C}$), insulation plate (4 cm thick), convergence guide ($l = 0.7$ m), $V_L = 5000$ m/min.

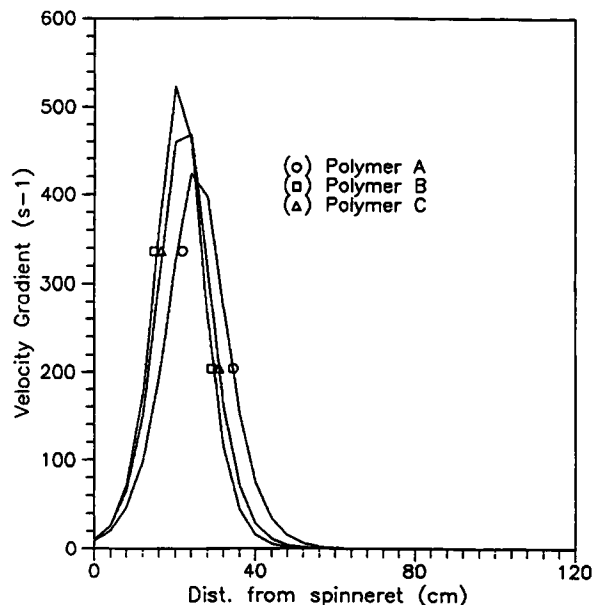


Figure 16 Threadline velocity gradient profile (calculated) of different PET polymers. $T = 295^\circ\text{C}$, sp. 14×0.23 mm ($L = 2.5D$), $L = 2.6$ m, without quench/heating, insulation plate (4 cm thick) plus convergence guide ($l = 0.7$ m), $V_L = 5000$ m/min, dpf = 1.43.

air friction contribution in multifilament spinning, in which case the effect of the convergence guide on the stress would have to be considered.

Figure 17 shows that the spinline stress level is lowered with the use of the heating device, insulation plate, or convergence guide. The spinline stress level is greatly reduced with the simultaneous use of the convergence guide and insulation plate. This figure also demonstrates the importance of the air friction contribution for the finer fibers, as indicated by the linear portion of these curves, in which cases a more realistic picture would require considering the effects of air drag in multifilament spinning. The comparison of the spinline stress level of fibers from the three polymers is shown in Figure 18. It can be seen that fibers from polymer A show the lowest stress level. The stress level of fibers from polymers B and C may be considered similar.

The cooling rate is reduced with the simultaneous use of the insulation plate and convergence guide but not as much as when only the heating device is used, as shown in Figure 13. Therefore the lower value of the minimum denier in this case is due not only to the reduced cooling rate, but also to the level of the spinline stress. The level of the spinline stress is shown in Figure 17 to be much lower in the case of simultaneous use of the insulation plate and convergence guide than in the case of using the heating

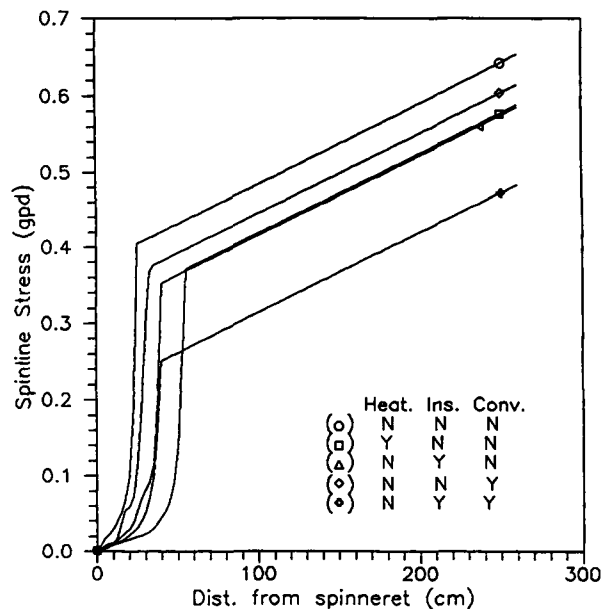


Figure 17 Threadline stress profile (calculated) of polymer A with varying spinline modifications. $T = 295^{\circ}\text{C}$, sp. $14 \times 0.23 \text{ mm}$ ($L = 2.5D$), $L = 2.6 \text{ m}$, without quench, heating ($H = 20 \text{ cm}$, $Z = 15$ / $T = 180^{\circ}\text{C}$), insulation plate (4 cm thick), convergence guide ($l = 0.7 \text{ m}$), $V_L = 5000 \text{ m/min}$, $\text{dpf} = 1.43$.

device only. The improved stability of the threadline associated with the lower air drag due to the convergence may also have an important effect on the minimum denier attainable. The insulation plate may have the effect of a delayed quench while the convergence guide would have the same effect as reducing the threadline length and at the same time reducing the bundle turbulence. It is worth mentioning that the use of a convergence guide as a means to reduce the threadline length affords greater flexibility to existing installations as compared to actually bringing the winder closer to the spinneret.

Figures 19 and 20 show the calculated spinline viscosity for the same spinning conditions presented in Figures 17 and 18, respectively. Due to the approximations involved in the previous calculations of the spinline stress and velocity gradient, these results should be used only to show general trends. The first trend to be observed is the several order of magnitude change of the spinline viscosity along each respective threadline. This shows that the spinline viscosity is much more dependent on the threadline temperature than on the strain rate, since we would expect from the latter less than one order of magnitude change of the apparent elongational viscosity in the range of strain rate encountered in

the present spinning conditions, as presented in the earlier paper.⁵

The results of the spinline viscosity shown in Figures 19 and 20 reflect the cooling conditions, where the level of the spinline viscosity increases with a faster threadline cooling. The comparison of the spinline viscosity for the three polymers in Figure 20 shows once more that polymer B has the highest viscosity level, followed by polymers C and A.

The larger dependence of spinline viscosity on the threadline temperature than on the strain rate could lead to the conclusion that the strain rate dependency of the elongational viscosity is not important in determining the spinline stress level and the limit of the fine denier. However, we have shown that the threadline diameter profile and the minimum denier coincide with the level of the apparent elongational viscosity data determined from the Instron rheometer tests. We speculated that both the strain rate dependency and the level of the apparent elongational viscosity are important in determining the spinline deformation in the region close to the spinneret. In this region, due to the higher spinline temperatures, the initial deformation rate and apparent elongational viscosity level will be the main parameters in determining the spinline stress. Dif-

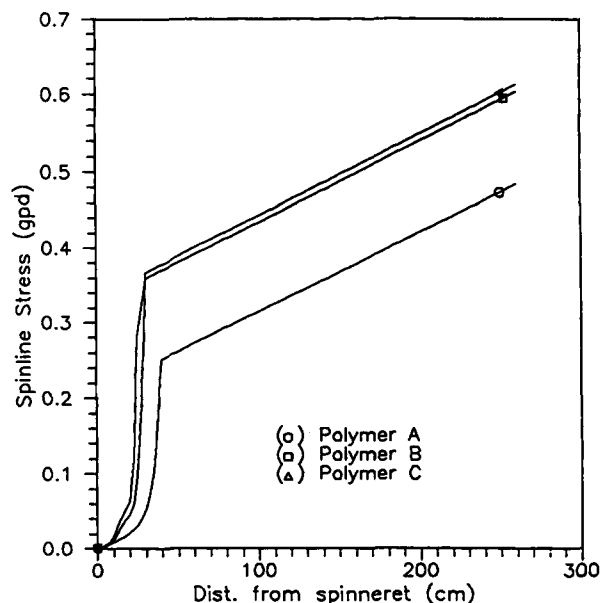


Figure 18 Threadline stress profile (calculated) of different PET polymers. $T = 295^{\circ}\text{C}$, sp. $14 \times 0.23 \text{ mm}$ ($L = 2.5D$), $L = 2.6 \text{ m}$, without quench/heating, insulation plate (4 cm thick) plus convergence guide ($l = 0.7 \text{ m}$), $V_L = 5000 \text{ m/min}$, $\text{dpf} = 1.43$.

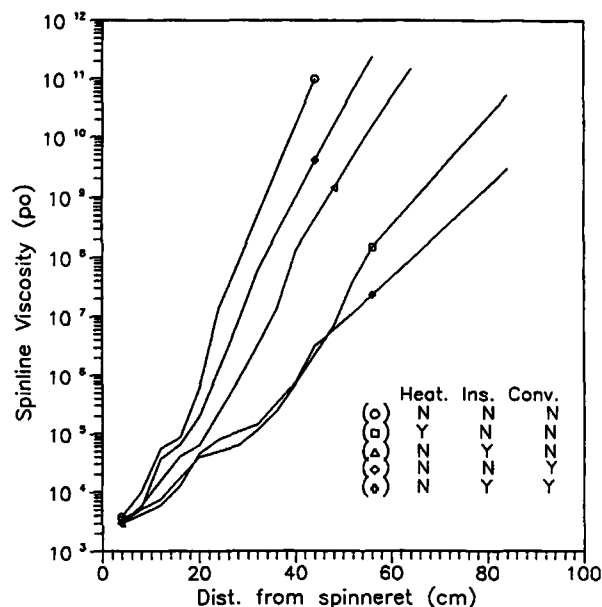


Figure 19 Spinline viscosity profile (calculated) of polymer A with varying spinline modifications. $T = 295^{\circ}\text{C}$, sp. $14 \times 0.23 \text{ mm}$ ($L = 2.5D$), $L = 2.6 \text{ m}$, without quench, heating ($H = 20 \text{ cm}$, $Z = 15/T = 180^{\circ}\text{C}$), insulation plate (4 cm thick), convergence guide ($l = 0.7 \text{ m}$), $V_L = 5000 \text{ m/min}$, $\text{dpf} = 1.43$.

ferent deformation rates result in different cooling rates. The threadline temperature then will have the major effect on the spinline viscosity. Therefore we may conclude that the determination of the strain rate dependency of the apparent elongational viscosity from the experiments done on the Instron capillary rheometer is important in characterizing the elongational flow behavior of the different polymers, which can be correlated with the limiting conditions in the spinning of fine denier fibers.

Cold-Drawing Effects during the High-Speed Spinning of Fine Denier PET Fibers

It was mentioned earlier that the air drag provides the major contribution to the spinline stress, particularly for the very fine fibers. Fujimoto et al.¹⁸ reported that in some cases cold drawing between the solidification point and the take-up roller may occur. Cold drawing would be expected, according to their study, in the speed range of 4000–5000 m/min and take-up denier below 1. In order to verify the occurrence of cold drawing in our spinning system, samples of the 0.56 dpf fiber spun at 5000 m/min with the insulation plate and convergence guide were excised from the threadline. Figure 21 presents the results of birefringence and diameter of the ex-

cised samples in the region between the convergence guide, 70 cm from the spinneret, and the take-up roller, for two threadline lengths, 2.6 and 1.6 m. It can be concluded from these results that no additional stretching of the fibers occurs with the longer threadline, and the fiber orientation and diameter are essentially constant after the convergence guide down to the take-up device.

Cold drawing was, however, observed if the fibers were taken-up at the winder and the threadline length was increased to 5 m. Additional tension was imposed by a spin finish applicator 1 m from the spinneret and by friction in the traverse guide. Table V compares the results of birefringence of the fibers collected on the godet rolls (2.6-m-long threadline) and on the winder (5-m-long threadline) with different take-up denier and speed.

As shown in Table V, cold-drawing effects, as indicated by the increase in birefringence, are more severe in the finer denier fibers and lower spinning speed. A value of yield stress for cold drawing of 0.5 gpd was reported by Cheng et al.¹⁹ This value seems to be extremely low, since even the 1.5 dpf fibers would be cold drawn at 5000 m/min from the results of take-up stress shown in Figure 7, which was not observed. As shown in Table V cold drawing was observed only for the fibers collected on the winder at 5 m from the spinneret and with additional ten-

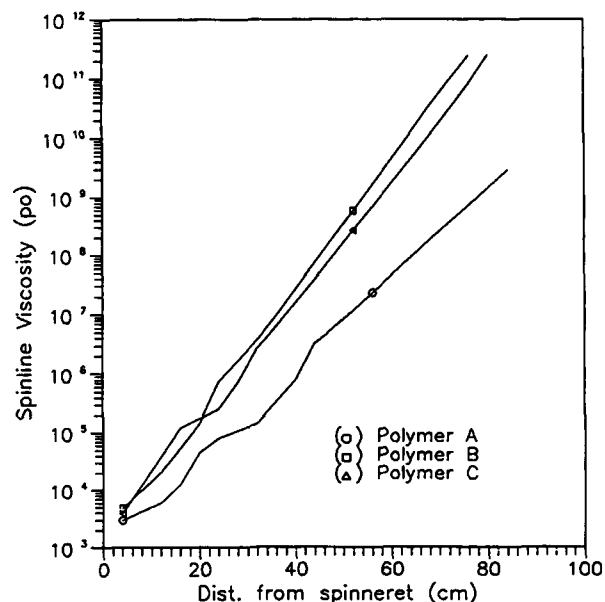


Figure 20 Spinline viscosity profile (calculated) of different PET polymers. $T = 295^{\circ}\text{C}$, sp. $14 \times 0.23 \text{ mm}$ ($L = 2.5D$), $L = 2.6 \text{ m}$, without quench/heating, insulation plate (4 cm thick) plus convergence guide ($l = 0.7 \text{ m}$), $V_L = 5000 \text{ m/min}$, $\text{dpf} = 1.43$.

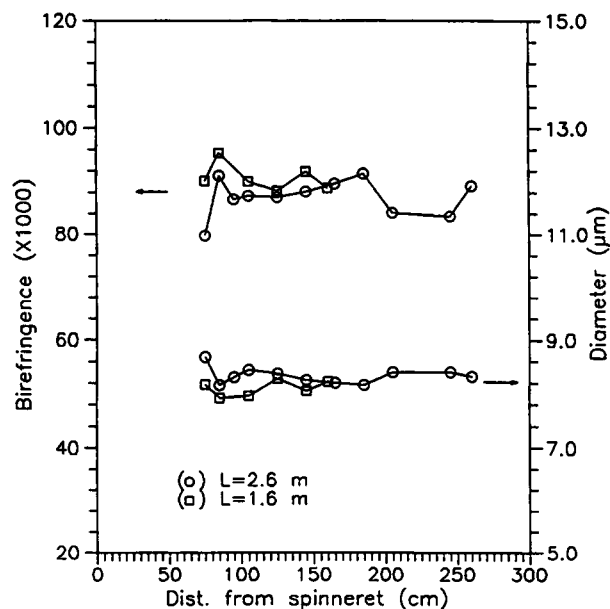


Figure 21 Birefringence and diameter profile of samples of polymer A excised from the threadline. $T = 295^{\circ}\text{C}$, sp. $14 \times 0.23 \text{ mm}$ ($L = 2.5D$), without quench/heating, insulation plate (4 cm thick) plus convergence guide ($l = 0.7 \text{ m}$), $V_L = 5000 \text{ m/min}$, dpf = 0.56.

sion from the finish applicator and traverse guide. Ziabicki¹ reports a value of $5 \times 10^9 \text{ dyn/cm}^2$ (4 gpd) as the yield stress for the cold drawing of PET. This value is much higher than the take-up tension results shown in Figure 7, and therefore one should not expect cold drawing to occur in the spinning conditions indicated in Tables III and IV.

Cold drawing effects, reported by Fujimoto et al.¹⁸ for fibers spun at speeds in the range of 4000–5000 m/min and take-up denier below 1, were not observed in our experiments at 5000 m/min and take-up denier of 0.56, as shown in Figure 21. We attribute these discrepancies to the higher level of stress in their study due to the unusual long threadline used (4.7 m) as well as to the absence of the spinline devices aimed at reducing the stress level, such as the insulation plate and convergence guide used in the present research.

CONCLUSIONS

It has been shown that elongational viscosity of the polymer is the key parameter affecting the attainment of fine denier fibers. Low IV polymers have lower elongational as well as lower shear viscosities, and they are more suitable for obtaining fine denier fibers compared to high IV polymers. When poly-

mers have similar shear viscosities, the polymer with the lower elongational viscosity permits spinning of finer denier fibers. This result has been attributed to lower spinline tension generated when spinning lower elongational viscosity polymers.

Besides the polymer characteristics just discussed, the spinning conditions are also important to the attainment of the minimum take-up denier. The effects of the take-up velocity, threadline length and quenching conditions have been studied. For the low IV polymers, the effects of take-up speed and threadline length are small up to the speed of 4000 m/min, and take-up denier lower than 0.5 has been obtained even without the use of quenching and/or heating devices. Fiber denier as low as 0.22 dpf was obtained at the spinning speed of 4000 m/min. For the high IV polymer the shorter threadline made possible the spinning of finer denier fibers at all take-up velocities, especially at 5000 m/min. It is only at 5000 m/min that the effect of the threadline length becomes important in the case of low IV polymers, and in addition the difference among the polymers becomes more significant. At this speed take-up denier less than 1 dpf can be obtained only when a heating device is used to slow down the threadline cooling, but significant reduction of the limits of the minimum denier was obtained only with the simultaneous use of an insulation plate and convergence guide. The use of both devices, in addition to selection of the optimum spinneret capillary diameter and proper filtration of the polymer melt, allowed spinning of the remarkable low value of 0.38 dpf at the high spinning speed of 5000 m/min. The lower spinline stress level obtained with the use of these devices also avoided cold-drawing effects during the spinning of the fine denier fibers.

The use of the insulation plate and convergence guide are cited frequently in the Japanese patent literature, but either they are not used in combination or the spinning speeds used are much lower than those employed in this study. Also no descrip-

Table V Cold-Drawing Effects of Fibers Spun from Polymer A

Take-up Speed (m/min)	dpf	Birefringence ($\times 10^3$)	
		Godet	Winder
4000	1.00	64.3	76.2
	0.22	86.8	124.7
5000	1.00	89.3	107.4
	0.38	94.8	125.9

tion is given of the effects on the threadline dynamics. In this report we presented several results of the study of the threadline dynamics as modified by these devices.

The results of the threadline dynamics analysis show that the cooling rate is slowed with the convergence guide in place and this effect is larger when the insulation plate is used. The cooling rate is further slowed down when the insulation plate is used simultaneously with the convergence guide. However, the cooling rate when the insulation plate is used simultaneously with the convergence guide is still faster than the cooling rate when only the heating device is used. Therefore the cooling rate is not the only parameter influencing the lower limit of the spun denier. Stress profile data show that the reduction of the spinline stress level is greatly enhanced with the simultaneous use of the insulation plate and convergence guide, compared with the reduction attained with the use of the heating device, insulation plate, or convergence guide alone. This reinforces the conclusion that the spinline stress is the most important parameter in determining the fine denier limit. It is affected by the cooling profile, the elongational flow properties of the polymer as well as the air drag generated in the spinline, which is the most important term determining the spinline stress level due to the very fast cooling of the fine denier fibers. It should be added that the use of the convergence guide, besides having the same effect of reducing the air friction as is experienced in a shorter threadline, also contributes to impart stability to the threadline, which becomes less sensitive to the turbulences caused by the surroundings.

The trends shown by the spinline viscosity profiles indicate that temperature is the most important parameter determining the viscosity values, while the strain rate dependency of the apparent elongational viscosity has only a negligible effect. However, the elongational flow characteristics determined from the Instron rheometer tests could be correlated with the threadline diameter profile and the minimum denier attainable in the spun fibers, and therefore the apparent elongational viscosity data obtained with the Instron capillary rheometer are still important in predicting the fine denier melt-spinning behavior.

The properties of the fine denier fibers may be

equivalent to the 1 dpf fiber spun at a speed 1000 m/min higher, as a consequence of the higher orientation observed in the finer denier fibers. The similarity of the effect of increase of the take-up speed or decrease of the take-up denier on fiber orientation, as well as other microstructure features, will be analyzed in more detail in a subsequent study.

The authors wish to acknowledge the financial support received from Rhodia S.A.

REFERENCES

1. A. Ziabicki, in A. Ziabicki and H. Kawai, Eds., *High Speed Fiber Spinning*, Wiley, New York, 1985, Chapter 2.
2. A. Ziabicki, *Fundamentals of Fiber Formation*, Wiley, New York, 1976.
3. R. Beyreuther and A. Schöne, *Acta Polym.*, **34**(2), 68–72 (1983).
4. W. Qiu, *J. China Textile Eng. Assoc.*, **6**(9), 534–536 (1985).
5. C. T. Kiang and J. A. Cuculo, *J. Appl. Polym. Sci.*, **46**, 55–65 (1992).
6. G. Y. Chen, Ph.D. Thesis, Fiber and Polymer Science Program, North Carolina State University, Raleigh, 1990.
7. M. Matsui, in A. Ziabicki and H. Kawai, Eds., *High Speed Fiber Spinning*, Wiley, New York, 1985, Chapter 5.
8. S. Kase and T. Matsuo, *J. Appl. Polym. Sci.*, **11**, 251–287 (1967).
9. H. M. Laun and H. Schuch, *J. Rheology*, **33**(1), 119–175 (1989).
10. Unitika, JPA 54-73,915 (13 June 1979).
11. Unitika, JP 60-51,561 (14 November 1985).
12. Toray, JP 61-14,243 (17 April 1986).
13. Teijin, JPA 61-186,515 (20 August 1986).
14. Asahi, JPA 55-26,201 (25 February 1980).
15. Asahi, JPA 55-132,708 (15 October 1980).
16. Japan Ester, JPA 56-31,007 (28 March 1981).
17. Kanebo, JPA 56-63,008 (29 May 1981).
18. K. Fujimoto, K. Iohara, S. Owaki, and Y. Murase, *Sen-i Gakkaishi*, **44**(10), 477–482 (1988).
19. J. Cheng, X. Guan, R. Wei, and H. Ma, *Intern. Polym. Process.*, **III**(2), 95–99 (1988).

Received October 29, 1991

Accepted November 4, 1991